International Journal of Coal Geology 172 (2017) 31–42

Contents lists available at ScienceDirect

International Journal of Coal Geology

journal homepage: www.elsevier.com/locate/ijcoalgeo

Key strata characteristics controlling the integrity of deep wells in longwall mining areas

Shun Liang [a,b,c], Derek Elsworth [b], Xuehua Li [c,*], Xuehai Fu [a], Boyang Sun [c], Qiangling Yao [c]

[a] Key Laboratory of Coalbed Methane Resource and Reservoir Formation Process, Ministry of Education, China University of Mining and Technology, Xuzhou, Jiangsu 221008, China
[b] EMS Energy Institute, G3 Center and Energy and Mineral Engineering, Pennsylvania State University, University Park, PA 16802, USA
[c] School of Mines, Key Laboratory of Deep Coal Resource Mining, Ministry of Education, China University of Mining and Technology, Xuzhou, Jiangsu 221116, China

ARTICLE INFO

Article history:
Received 22 August 2016
Received in revised form 24 January 2017
Accepted 24 January 2017
Available online 3 February 2017

Keywords:
Strata combination
Longwall mining
Oil/gas well
Shale gas
Well integrity

ABSTRACT

The damage of vertical oil/gas wells in longwall mining areas is mainly a result of strata movement induced by coal extraction. Strata with contrasting lithology vary dramatically in their movement and potential for well damage, with some special combinations of strata in particular having the greatest potential for damage. This study investigates the effects of specific combinations of strata transition structures ((i) topsoil-bedrock, (ii) a thin weak interlayer sandwiched above and below by two stiff beds, and (iii) the key-stratum sandwiched above and below by two soft beds) on the magnitude, severity and distribution of various anticipated well deformations, and explores the optimal drilling path for wells to maximize well integrity. Results indicate that: (1) Effects of various combinations of strata on well deformation lie essentially in the mismatch in the mechanical properties of the strata and weak interfaces, with the stratum thickness and vertical distance from the coal seam to the stratum/interface also exerting a significant influence. (2) Wells in the upper part of the topsoil are subject to horizontal tension, while the lower part is laterally compressed following the extraction of either one panel or both panels. Large lateral tensile strains normally arise at the upper part of the hard strata which directly underlie the soft strata. Large lateral compressive strains are concentrated in the strata within ~5 m above and below the coal seam and peak in the seam. Longitudinal well deformation is dominated by compression in soft strata, especially in the upper part of the layer, and is dominated by tension in stiff strata, within the lower portion in particular. Vertical compression at the interface is larger below the key-stratum, and peaks at the interface between the coal seam and its immediate roof. Well distortions in soft strata are 3 to 5 times those of ones in stiff strata. (3) Well deformations developing both at interfaces and within layers significantly intensify in the vicinity of the seam. An integrated consideration of various deformations of five candidate well paths indicates that the optimal position for well stability is the one that deviates from the pillar centerline and is close to the second mined panel.
© 2017 Elsevier B.V. All rights reserved.

1. Introduction

In the last two decades, the extraction of unconventional hydrocarbon resources (e.g., shale gas, shale oil, tight sandstone gas, etc.) has developed rapidly. However, in some sedimentary basins where coal, gas and oil coexist, ensuring the stability of wells traversing longwall-mineable coal seams is becoming a barrier impeding their simultaneous recovery (Liang et al., 2014; Rostami et al., 2012; Su, 2016; Scovazzo and Russell, 2013; Wang et al., 2013). The extensive and intense strata movement and deformation induced by the longwall mining of coal may leave the upper vertical sections of oil/gas wells vulnerable to failure by shear, compression and other deformations. This susceptibility of well survivability has significant implications on cost (Chen et al., 2012; Dodson, 2004; Yan et al., 2013; Zeynali, 2012; Zhang et al., 2009) and on safety (Miyazaki, 2009; Rice and Hood, 1913; Vidic et al., 2013; Zabetakis et al., 1972; Zhai et al., 2015).

Resulting from the simultaneous recovery of coal and hydrocarbon resources, the importance of well survivability has been noted since the early 20th century (Rice and Hood, 1913). It was not until the early 1970s that the longwall method of coal mining gained popularity due to its higher productivity and low cost. In the past two decades, an expansion in the exploitation of unconventional hydrocarbon resources has resulted in the stability of wells piercing longwall-minable coals becoming a key issue. Some (Luo et al., 2002; Peng et al., 2003; Scovazzo and Russell, 2013) believe that factors, including the coal seam burial depth, mining-induced stresses, coal pillar dimensions, and relative position of the well and coal face, should be considered during the design of coal pillars reserved for well conservation. Mining-induced strata deformation and coal strength are vital in understanding strata deformation and its impact on well stability. The identification of the instability mode of well casings is a prerequisite for the determination of the strata deformation and the ultimate impact on casing. Using

* Corresponding author.
E-mail address: lsxh2001@126.com (X. Li).

http://dx.doi.org/10.1016/j.coal.2017.01.012
0166-5162/© 2017 Elsevier B.V. All rights reserved.

numerical simulation, Rostami et al. (2012) and Wang et al. (2013) investigated the axial distribution of stress, strain, and displacement along shale gas wells. In their research, the strata are first arranged homogeneously and then alternately with the use of soft and hard beds, failing to take the effect of slidable interfaces and different strata combinations into account. In the Ordos basin, China, also, the simultaneous exploitation of coal and hydrocarbon resources compete with each other. The abandoned oil/gas wells are ordinarily plugged at the surface, cut underground, or advanced through directly by the coal face. Fig. 1 shows 2#, 3#, and 7# abandoned oil wells exposed at a longwall working face and in the gateroad of the Hecaogou colliery in the Ordos basin. While for producing wells, coal pillars are preserved around the wells in advance, and the coal panels have to be rearranged – reducing production efficiency. So far, little work examines the stability control of wells in longwall mining areas, despite some papers (Rice and Hood, 1913; Wang et al., 2014; Yun, 2014) introducing the hidden hazards and construction difficulties during the excavation of wells through the coal seam and the gob.

Further investigations have defined and then investigated the effect of key factors influencing the stability of gas wells as they traverse mineable coal seams. The factors examined include topography, coal seam burial depth, the presence of weak interfaces between alternating soft and stiff layers, and sequential extraction of coal faces on both sides of well-protecting coal pillars (Liang et al., 2014; Liang et al., 2015a; Liang et al., 2015b), applied principally to seams in southwest Pennsylvania, USA. The strata deformation and movement caused by coal extraction is a dynamic mechanical process propagating upwards (Karacan et al., 2007; Karacan, 2015; Palchik, 2003; Preusse, 2001; Qian, 1996; Schatzel et al., 2012). Coal measure strata typically are composed of numerous bedded sedimentary formations of varying strength, stiffness and thickness. Therefore, apart from the mechanical properties of strata, interfaces between layers and layer thickness (Fan and Zhang, 2015; Ghazvinian et al., 2010; Karacan, 2009, 2015; Karacan and Goodman, 2009; Lu et al., 2016; Majdi et al., 2012; Palchik, 2003, 2005; Richard et al., 1990; Su, 2016; Whittles et al., 2006), the combination sequences of soft and hard layers, which have not aroused adequate attention, also significantly affect the movement and deformation of the overburden, and the resulting deformation and performance of hydrocarbon wells, gob gas ventholes (GGVs) and methane production boreholes which penetrate the overlying strata (Huang, 2010; Karacan, 2009, 2015; Karacan et al., 2005, 2007, 2011; Sun, 2008; Xu et al., 2011). This paper examines the deformation of vertical gas wells in longwall mining areas under different combinations of strata sequences. More specifically, the effects of topsoil-bedrock, hard-soft-hard (HSH) strata structures, and soft-hard-soft (SHS) strata structures and interfaces within these strata combinations are examined with respect to well deformation (including shear, distortion, tension and compression). This study is a follow-up of the previous investigation made by Rostami et al. (2012), Liang et al. (2014), Liang et al. (2015a) and Liang et al. (2015b).

2. Establishment of the geologic model

In this work, the geologic model is examined with a two-dimensional continuum finite difference program, representing deformable strata and "interfaces".

2.1. Deformation of strata and oil/gas wells

We follow (1) the horizontal shear slippage and vertical compression occurring at interfaces between alternating layers, (2) axial distortion and, (3) tension and compression occurring within layers both in the horizontal and vertical directions. These deformations represent the anticipated failure mode for oil/gas wells that pierce the intervening coal protective pillars between longwall panels (LWPs). These pillars are part of typical panel development plans (3 entry gates) and include a set of two pillars between LWPs (Fig. 2). We represent the interface between layers of alternating mechanical properties by an interface element (Fig. 3) where the elastic distortion, ε_e, irrecoverable shear slip distortion, ε_i, and total distortion, $\varepsilon_t = \varepsilon_e + \varepsilon_i$ are defined as (Fig. 3):

$$\begin{aligned} \varepsilon_e &= \frac{U_x}{d} = \frac{U_{ij} - U_{i(j-1)}}{d} \\ \varepsilon_i &= \frac{\Delta U}{\Delta d} = \frac{U_{i(j+1)} - U_{ij}}{\Delta d} \\ \varepsilon_t &= \frac{T_x}{d} = \frac{U_{i(j+1)} - U_{i(j-1)}}{d} \end{aligned} \tag{1}$$

in terms of elastic shear offset, U_x, relative slip offset, ΔU, total offset, $T_x = U_x + \Delta U$ and normalized over the bed thicknesses, d or Δd, referring to the separating distance between layers. U_{ij} refers to the lateral shear displacement of node (i, j), with a similar meaning for $U_{i(j\text{-}1)}$ and $U_{i(j+1)}$ (Fig. 3).

2.2. Failure criterions of strata and interfaces

The Mohr-Coulomb criterion, is applied as the strata yield criterion,

$$\tau = c + \sigma_n \tan\phi \tag{2}$$

where the cohesion (c) and internal friction angle (ϕ) of the strata and interfaces are considered, linking shear strength (τ) to normal stress (σ_n).

A shear dislocation occurs along interfaces as the key factor inducing the shear and distortion of the well. The FLAC model comprises two types of interfaces formed by soft and hard strata, which is distinguished by Eqs. (3) and (4) (Itasca Ltd., 2002).

Fig. 1. Images taken underground for three abandoned oil wells exposed at the lomgwall working face (a, b) and in the gateroad (c) of Hecaogou colliery in the Ordos basin, China.

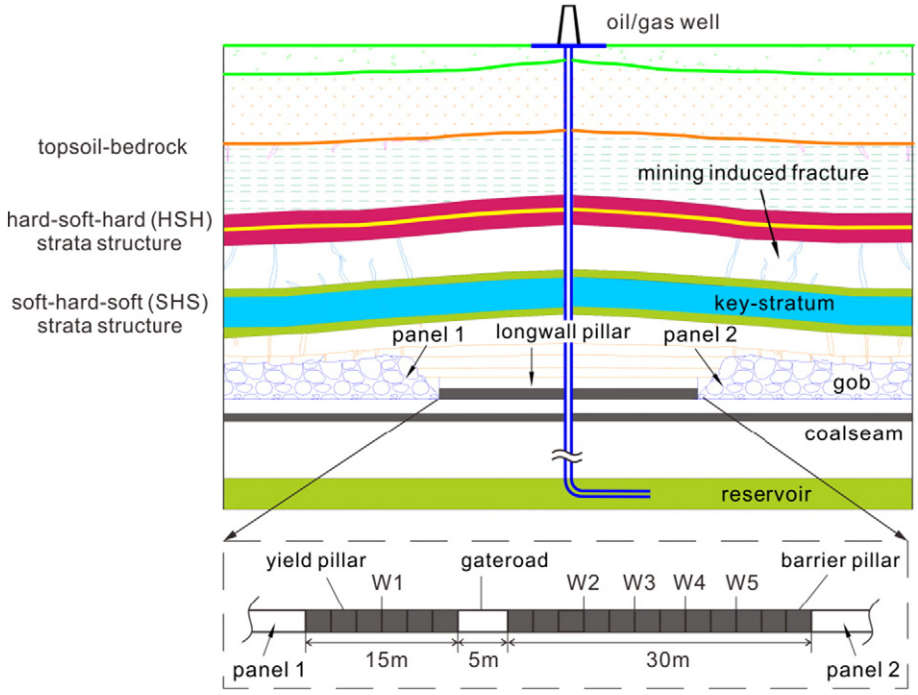

Fig. 2. The two-dimensional geological model of one vertical oil/gas well penetrating longwall pillars.

(1) Coulomb criterion of shear strength

$$F_{\text{smax}} = c\ L + \tan\phi F_n \tag{3}$$

If $|F_s| \geq F_{\text{smax}}$ in Eq. (3), then $F_s = F_{\text{smax}}$, and the shear symbol is retained.

(2) Tensile yield criterion

$$F_t = \sigma_t - t \tag{4}$$

where σ_t is the tensile stress exerted on the interface, and t is its tensile strength (assumed zero in our model). If $F_t \geq 0$, then the interface will be pulled apart and the normal and tangential forces are reset to zero.

2.3. Selection of simulation parameters

The mechanical parameters of the strata and interfaces dictate the shear, tensile, and compressive deformation and distortion arising in the wells. The authors have already explored the sensitivity of well deformations to these mechanical parameters involving Young's modulus, E; Poisson"s ratio, μ; cohesion, c; internal friction angle, ϕ; and of interfaces including shear stiffness, K_s; normal stiffness, K_n; internal friction angle, φ, with the conclusions defined as below (Liang, 2015):

(1) Horizontal shear offset and vertical compression occurring at interfaces between alternating layers of hard and soft strata are not sensitive to the difference of Young's moduli of adjacent strata, and are only weakly sensitive to contrasts in Poisson ratios. As Poisson"s ratio increases, the horizontal shear and vertical compression increases slightly and linearly.

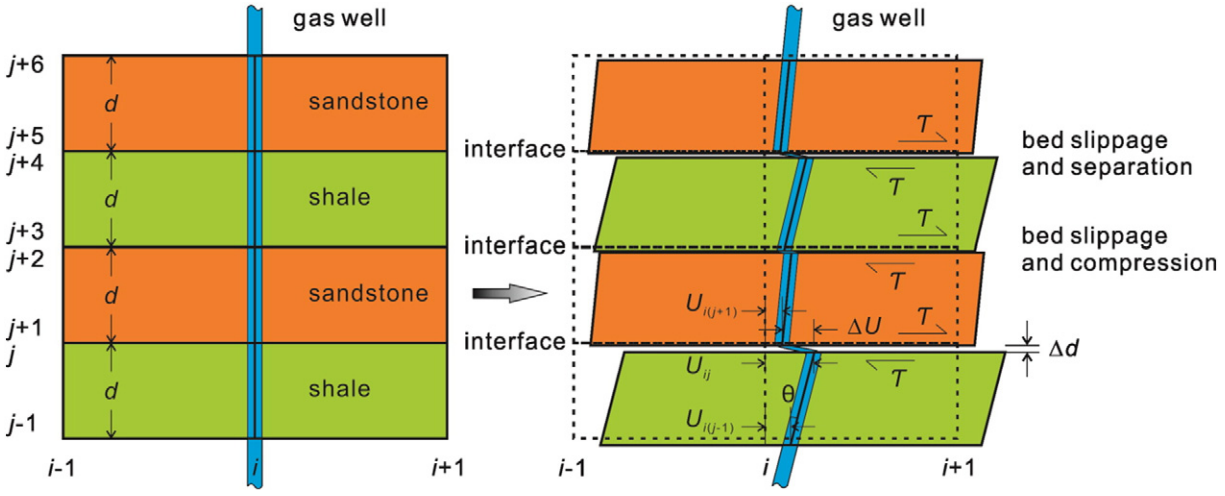

Fig. 3. Typical deformation of a well in and between layers of alternating soft shale and stiff sandstone as the well is distorted by the strata after coal mining (with slip interfaces between alternating layers) (Liang et al., 2014).

(2) Horizontal shear offset and vertical compression occurs at interlaminar interfaces and these are insensitive to the cohesion and internal friction angle of adjacent strata. In comparison with the vertical compression at weak interfaces, the horizontal shear offset is susceptible to the difference of tensile strengths of adjacent strata.
(3) Horizontal shear offsets and vertical compression which occurs at weak interfaces between alternating layers is critical for well integrity. These offsets are largely dominated by the shear stiffness, normal stiffness, and internal friction angle of the interface (K_s, K_n, and φ), conforming to a logarithmic relation. This sensitivity weakens logarithmically with an increase in the stiffness and internal friction angle of the interfaces. When K_s and $K_n < 25$ MPa and $\varphi < 15°$, the well deformations at these interfaces increase dramatically, and are only marginally influenced by the properties of the intact strata.

We take this understanding of the key influences of strata response and its dependence on key properties to define the key combinations of strata properties implicated in well failures. As noted above, these focus on the properties of the interfaces, and the combination of soft or stiff layers above and below. Based on this, we examine these key combinations accommodating the mechanical parameters for the strata and interfaces in a numerical model (Fig. 2), as listed in Tables 1 and 2 (Rueda et al., 2014; Sun, 2008; Wang et al., 2012), in which K is the bulk modulus, G is the shear modulus, ρ is dry bulk density, *and* σ_t is the tensile strength. The 2D model is 2000 m × 607.3 m in vertical section and comprises overburden (305.3 m), coal seam (2 m) and underburden materials (300 m). Within the overburden, the topsoil is 80 m in thickness, the weak interlayer is 0.3 m thick and is sandwiched above and below by two hard sandstones (15 m), forming a hard-soft-hard (HSH) strata combination structure. The key-stratum (25 m) is positioned between two soft mudstones (5 m) to achieve a soft-hard-soft (SHS) strata combination structure. The remaining strata are divided every 10 m and alternate as soft and hard rock layers. Bed contacts between these layers are allowed to delaminate and slip. The LWPs are 370 m wide and are advanced into the page - in this 2D analysis, each panel is assumed to be excavated instantaneously and to infinite length - first on the left (panel 1), then subsequently on the right (panel 2).

The central pillar between panels is divided into a yield pillar (15 m wide), a barrier pillar (30 m wide) and contains three entries (each entry is 5 m wide). The roles of the pillars are to support the development phase of the panels, protect the longwall mining operation and related activities, especially ventilation, and to provide a smooth transition of the stresses of the upper strata between the panels. Wells are drilled vertically, penetrating the intervening pillars.

Table 2
The mechanical parameters of weak interfaces between layers in the numerical model.

Interface	K_s/MPa	K_n/MPa	φ/°
Topsoil-bedrock	15	15	20
HSH strata structure (weak interlayer)	24	24	20
SHS strata structure (key-stratum)	24	24	20
Coal seam-immediate roof	20	20	20
Coal seam-immediate floor	33	33	20
Sandstone-mudstone	29	29	25

3. Analysis and discussion of numerical results

We compare the impacts of longwall mining on well stability. In particular we examine the shear, tensile, and compressive deformation and distortion of wells excavated in various combinations of strata. Spatially, well deformation contains two parts, comprising deformation within the strata and at the interfaces between layers. The first part can be represented by horizontal, vertical, and shear strains. The second part is calculated by the horizontal and vertical relative motion of the strata directly above and below the interbed interface, which is characterized by both horizontal shear displacement and vertical compression.

In the numerical model, five measuring lines are arranged corresponding to the five schemes of well trajectories (W1 –W5) that penetrate the intervening pillars between panels (Fig. 2). In this analysis we neglect any added resistance applied by the well casing - as this resistance is trivial in comparison to the deformations applied by the strata. Peng et al. (2003) adopted the same approach in their global models. Consequently, we do not mesh the well, but use quantities (displacements and strains) of a series of nodes and zones which correspond to the five candidate vertical well trajectories to reveal the specific effect of strata structures on the magnitude and distribution of various well deformations. This is used to pinpoint the optimal drilling path that could benefit well integrity.

3.1. Magnitude and distribution of horizontal shear displacement

Figs. 4–8 illustrate the magnitude and distribution (1) of the horizontal shear offset and vertical compression at the interfaces and (2) of the shear, horizontal, and vertical strains within the strata for wells in five schemes as the LWPs flanking the single central pillar are sequentially mined. Notably, the left subfigures all conform to well deformations after the extraction of LWP 1, and the right subfigures represent deformations after LWP 2 is excavated.

The horizontal shear displacements (Fig. 4) are concentrated at two types of interfaces: the first is at roof interfaces within 30 m above the coal seam, and the second are interfaces formed in SHS strata structures. In contrast, the corresponding displacements for interfaces formed in

Table 1
Distribution (thickness) and rock mechanical parameters in the numerical modeling of the effects of strata combination types on stability of vertical oil/gas wells in longwall mining areas.

Stratum	Thickness/m	Cumulated height/m	K/GPa	G/GPa	ρ Kg/m^3	c/MPa	Φ/°	σ_t/MPa
Topsoil	80	607.3	0.8	0.4	2000	0.8	20	0
Sandstone	10	527.3	26.7	16	2500	100	30	3.0
Mudstone	10	517.3	3.3	2.0	2300	25	25	0.4
Sandstone	10	507.3	13.3	8.0	2500	60	30	3
Mudstone	10	497.3	3.3	2.0	2300	25	25	0.4
	20	487.3	Alternated by sandstone and mudstone, 10 m-thick for each					
Sandstone	15	467.3	26.7	16	2650	90	30	3.0
Mudstone (weak interlayer)	0.3	452.3	4.2	1.9	2300	21	25	0.4
Sandstone	15	452	26.7	16	2650	90	30	3.0
	40	437	Alternated by sandstone and mudstone, 10 m-thick for each					
Mudstone	5	397	6.7	4.0	2300	21	25	0.4
Sandstone (key-stratum)	25	392	44.4	33.3	2650	100	35	5
Mudstone	5	367	4.2	1.9	2300	21	25	0.4
	60	362	Alternated by sandstone and mudstone, 10 m-thick for each					
Coal seam	2.0	302	3.3	1.5	1500	1.5	25	0.1
	300	300	Alternated by sandstone and mudstone, 10 m-thick for each					

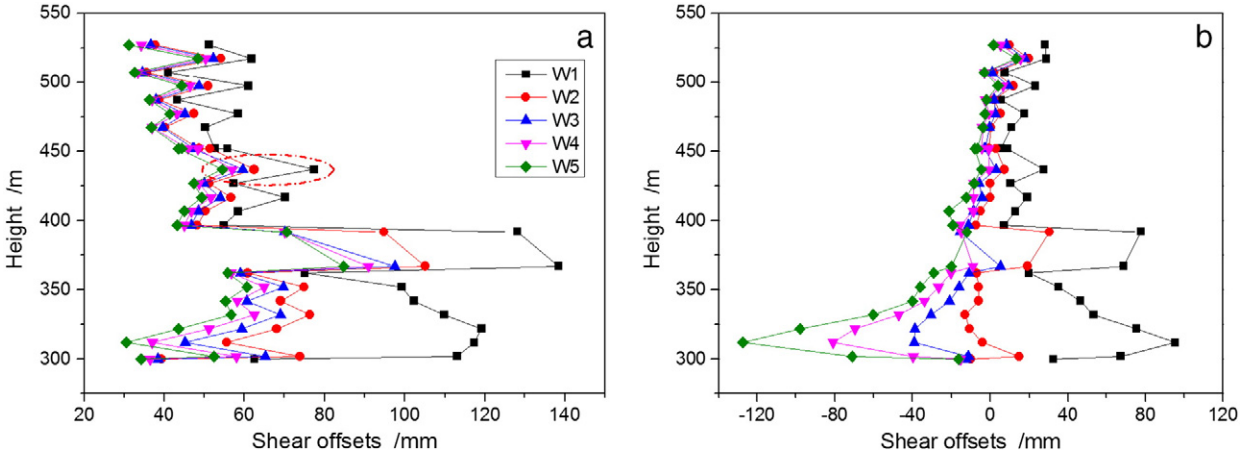

Fig. 4. Horizontal shear offsets of wells and their axial distribution affected by different types of strata combination.

topsoil-bedrock and HSH strata structures are negligibly small. Apparent from Tables 1 and 2 is that the topsoil-bedrock structure has the weakest interface in terms of its mechanical properties. A sensitivity analysis of well deformation identifies that interfaces with a lower stiffness are characterized by a higher shear displacement. However, this anticipated result is not found for the topsoil-bedrock interface, which indicates that a large mining-induced shear displacement is more likely to occur at the interface of SHS strata structures comprising a hard and thick layer (the key-stratum) than at the weak interface alone. Besides, the shear displacement at the interface in the HSH strata structure comprises a soft and thin layer and is small. Interestingly, larger lateral shear offsets also arise along the interface between the underlying hard sandstone (15 m) and the soft mudstone (10 m) both of which lie beneath the weak interlayer (0.3 m), as shown in the red dashed frame in Fig. 4(a). Consequently, it is inferred that larger shear slippage occurs along an interface sandwiched between an overlaying stiff layer and an underlaying soft layer, especially when the two adjacent layers are thick.

The interfacial shear displacement in the shallow roof, largely determined by the axial distribution of well shear displacement, is caused primarily by the high concentration of shear stress resulting from mining activities. The axial distribution of well shear displacement is also responsible for the insignificant shear displacement in the topsoil-bedrock and HSH strata interfaces, i.e., the shear displacement of interfaces is inversely related to its vertical distance to the coal seam because of the difference in intensity in the mining activities. After the extraction of panel 2, the horizontal shear offsets mainly concentrate at interfaces immediately above and below the key-stratum and at roof interfaces within 30 m of the coal seam. The interfacial shear displacements at other locations are all limited to only −25–30 mm. It can be concluded from the above analysis that a concentration of shear deformation, which innately threatens vertical well stability, is apparent at interfaces in the shallow roof and in the SHS strata structures. Especially for the strata structure with a hard thick layer overlying a soft thick one, similar phenomena have been observed at the weak interface between these two strata.

In the cross section of the pillar, horizontal shear offsets of well W1 are significantly greater than those of W2–W5 after LWP 1 is removed. In addition, W1 is at the left edge of the pillar and suffers the greatest from the excavation of panel 1. The peak shear offset of well W1 is 138.5 mm and occurs at the interface between the key-stratum and its immediate underlying mudstone. Shear offsets reduce monotonically as the well is positioned gradually farther from panel 1 (W2–W5, Fig. 2). After LWP 2 is mined, shear offsets rebound to some extent for most of the length of these 5 wells, while larger shear offsets still occur at interfaces formed in the SHS strata structure and in the shallow roof of the seam, with the greatest slippage being −127.3 mm (for well W5 which is closest to panel 2) and arising at the interface ~10 m above the pillar. Through an integrated consideration of shear offsets of these 5 wells after the twin LWPs are sequentially removed, well trajectory W3 may be the best drilling path for the well as its maximum shear offset is 97.5 mm after the removal of panel 1 and then changes to be −39.2 mm after the excavation of panel 2 – this is the least during the whole excavation of the LWPs. The maximum shear offset is also less than the threshold of the annular space (100 mm) between the production casing and the coal protection casing of the well (Liang et al., 2014). This

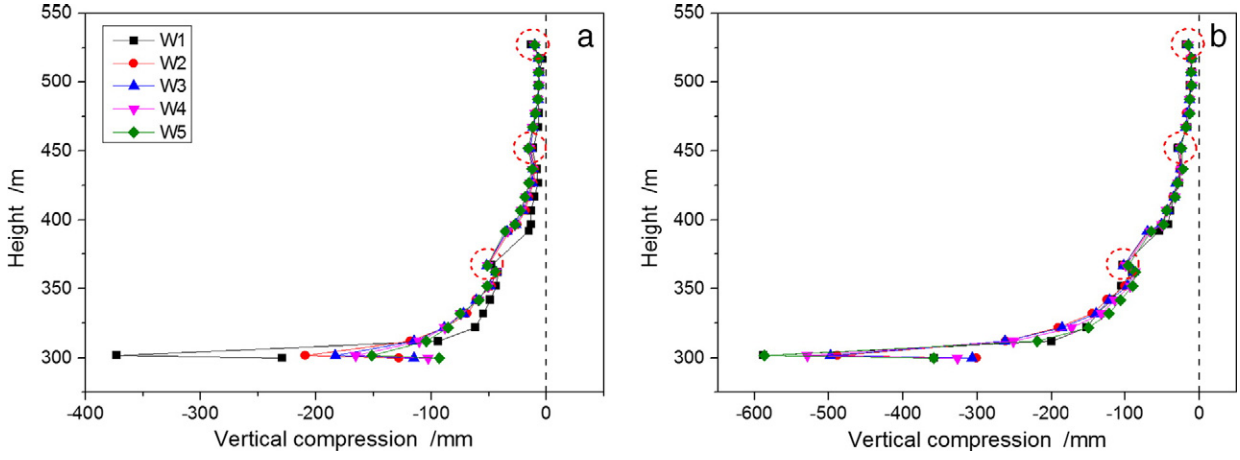

Fig. 5. Vertical compressions of wells between alternating layers and their axial distribution affected by different types of strata combination.

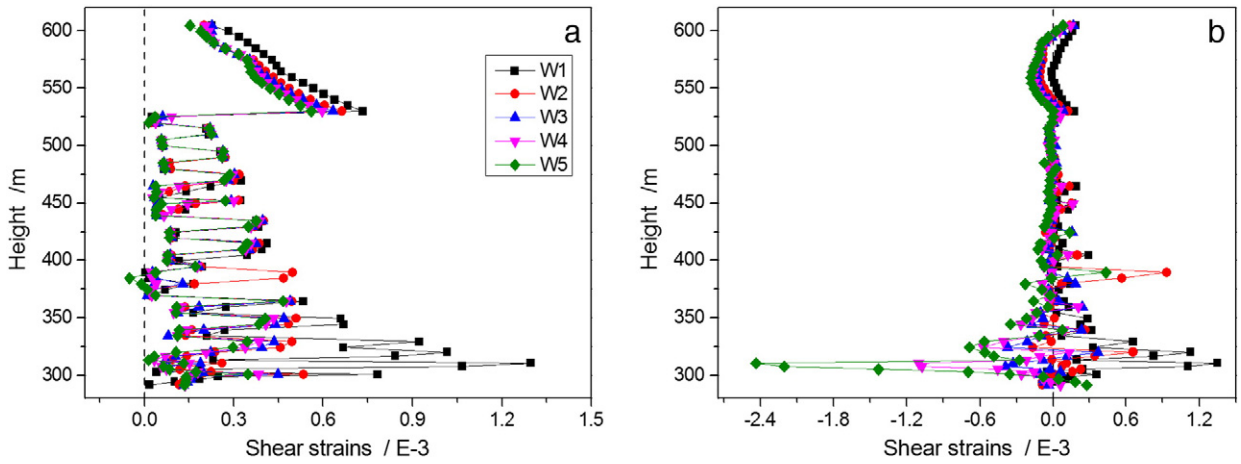

Fig. 6. Distortions of wells within the strata and their axial distribution affected by different types of strata combination.

threshold corresponds to the maximum allowable horizontal shear offset (both the positive and negative ones −±100 mm).

3.2. Magnitude and distribution of interface vertical compression

According to Fig. 5, the vertical compression at the interface below the key-stratum dominates the total amount of compression in the overlying strata. As the distance of the interface to the coal seam decreases, the interfacial compression rises dramatically, peaking at the interface directly contacting the coal seam. The key-stratum has a function of "isolating" the strata movement, i.e., it prevents the bending and subsidence of the underlying strata further transferring to its overlying strata. An upsurge in the vertical interfacial compression is detected at interfaces between (1) the key-stratum and the weak stratum directly below, (2) the weak thin stratum and the hard stratum immediately above, and (3) the topsoil and the bedrock, however, the increase is limited.

The extraction of panel 1 may significantly damage well W1, which is present in the yield pillar and closest to panel 1. The maximum interfacial compression for well W1 (−373 mm) is considerably higher than the other four wells (−151 –−209 mm). After the extraction of panel 2, the interfacial compression further rises as the subsidence of the overburden continues. For wells (W1 and W5) traversing the edges of the pillar, the peak interfacial compressions increase to −590 mm. For wells W2, W3, and W4, the vertical compression at the interface immediately above the coal seam is −488 mm, −498 mm, and −529 mm, respectively. When the bilateral LWPs are both removed, the gap between the vertical compressions of the five well schemes narrows. In addition, well W2, which is closest to the pillar center (Fig. 2), has the lowest vertical interfacial compression.

3.3. Magnitude and distribution of axial distortion

Fig. 6 indicates that larger axial distortions of wells caused by the extraction of panel 1 mainly take place at the bottom of the topsoil and in the shallow roof within 50 m of the coal seam. Since materials in the topsoil have uniform mechanical parameters, well distortion in the topsoil increases almost linearly before it enters the bedrock - this can be attributed to the stiffer/stronger mechanical properties of the hard bedrock (Table 1). Since the strata beneath the topsoil alternate as soft mudstones and stiff sandstones, the axial distortion of wells traversing these strata fluctuates. Well distortion within the soft strata surpasses those in the stiff strata, generally reaching 3 to 5 times the latter distortion. After the extraction of LWP 2, well distortions are partially restored for most of the length of the wells. Conversely, in the coal seam and its shallow roof, well distortions intensify due to the intense mining influence of LWP 2, reaching an order-of-magnitude of ~10^{-3}. These translate to shear offsets of ~1 and ~10 mm within one layer for bedding thicknesses of 1 m and 10 m, respectively. In summary, axial distortion of the wells is mainly related to the mechanical properties of the strata and the vertical distance to the coal seam. This trend is also affected by the combination types of the soft and hard layers.

Along the longitudinal direction, no evident increment in well distortion within the weak interlayer (mudstone, 0.3 m) is detected during the entire mining cycle. After panel 1 is removed, wells distortions in the key-stratum (sandstone, 25 m) are small except for well W2 which is on

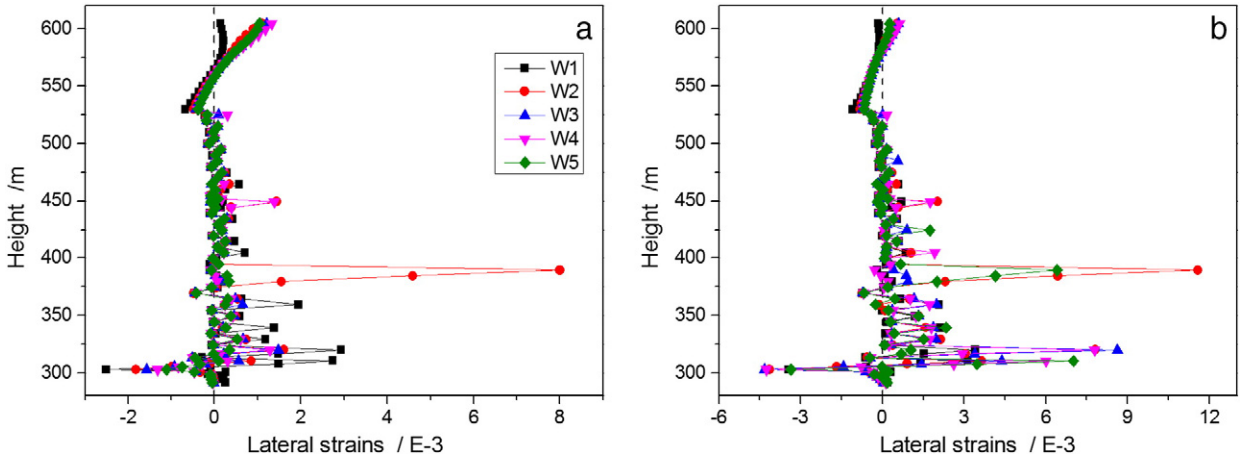

Fig. 7. Lateral strains of wells within the strata and their axial distribution affected by different types of strata combination.

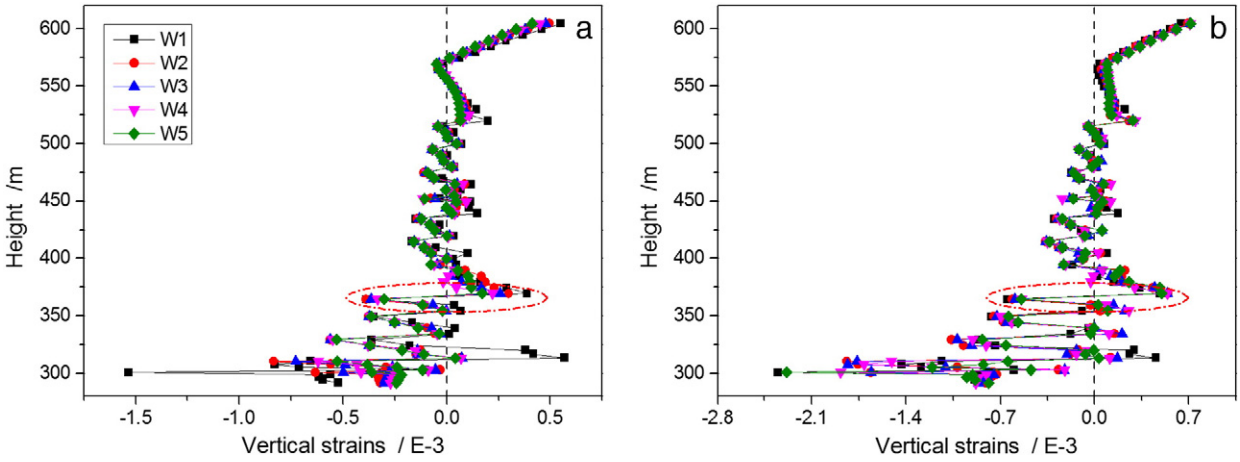

Fig. 8. Vertical strains of wells within the strata and their axial distribution affected by different types of strata combination.

the left edge of the barrier pillar. For wells traversing the edges of the barrier pillar (W2 and W5), axial distortions in the upper part of the key-stratum increase noticeably after the extraction of panel 2. While for well W1, which is closest to panel 1 and pierces the yield pillar, the distortion in the key-stratum remains entirely stable. It is surmised that well W1 in the key-stratum moves wholly towards the gob of panel 1 after the panel is removed, and that well W1 is distant from the edge of panel 2, whose mining-induced effect is markedly muted.

The above analysis identifies that the axial distortion of the well depends on strata mechanical properties and the vertical distance from the stratum to the coal seam. Specifically, wells traversing overlying weak strata and shallow roof above the seam are prone to large distortions.

3.4. Magnitude and distribution of the horizontal and vertical strains

Figs. 7 and 8 reveal the apparent effect of different strata structures (i.e., topsoil-bedrock, HSH, and SHS structures) on the magnitude and distribution of the horizontal and vertical strains. Specifically, the horizontal and vertical strains for wells within the topsoil change gradually until an abrupt variation at the interface between the topsoil and its underlaying bedrock. Lateral strains are dominated by tension for wells in the upper half of the topsoil, and compression for wells in the lower half. A small increase in lateral tensile strains occurs for wells W2 and W4 in the upper part of the 15 m thick sandstone immediately beneath the 0.3 m thick soft mudstone. A sharp rise in lateral tensile strains is apparent for wells W2 and W5, which pierce the edges of the barrier pillar, is detected in the upper part of this 25 m thick key-stratum after the twin panels are successively removed. Wells in the vicinity of the seam sustain the greater lateral strains both in extension (in the shallow roof of the seam) and compression (peaking in the seam).

Longitudinally, the vertical strain also fluctuates as the rock mechanical properties alternate between stiff and soft. Axial deformation in the soft strata is dominated by compression, which is especially true in the upper part of the soft layers. Vertical tension accounts for a major portion of the axial deformation of the well in hard layers, and in the lower part in particular. As the rock mechanical parameters and bed thickness differ widely (Table 1), the larger vertical tensile strains for wells in the lower part of the key-strata switch to larger compressive strains as the wells enter the upper part of the soft mudstone immediately below the key-stratum (Fig. 8). It is observed that the soft interlayer (mudstone, 0.3 m) is so thin that no apparent increase in vertical compressive strain is observed. Vertical strains are largest both at the surface where they are extensional and in the seam where they are compressive (Fig. 8). The peak vertical tensile and compressive strains are respectively limited to ~0.8 millistrain and ~−2.5 millistrain after the twin panels are mined. These are separately equivalent to vertical tensile and compressive displacements of <0.8 mm and 2.5 mm for a one meter length of the well. Lateral strains for wells within the strata are generally larger than vertical strains by roughly an order of magnitude (Figs. 7 and 8).

In conclusion, different combinations of strata sequences influence the magnitude and distribution of horizontal and vertical strains of the wells to various extents. The magnitude of well deformation within the layer is also determined by the layer thickness and the spacing between the layer and the coal seam. Even in the topsoil with uniform properties, the horizontal and vertical strains along the axial well are non-uniform. More specifically, wells in the upper part of the topsoil are subjected to horizontal tension, while those in the lower part are compressed. The shallow topsoil has a high vertical well deformation in tension.

4. Review and comparison with previous studies

Ensuring the stability of deep wells penetrating longwall-mineable coal seams is an urgent issue affecting the efficient co-extraction of the coal seam and the underlying hydrocarbon resources. This work explores the effects of strata combination structures on well stability. Substantially, studies on stability of underground openings (shafts, oil/gas wells, boreholes, gateroads/entries, caverns, et al.) and change of fluid conductivity over and around LWPs are all concerned with overburden subsidence caused by coal mining and the resulting strata deformation (bending, rotation, distortion, shear, separation and compression, et al.). Actual levels of distress experienced by wells undermined in the manner mentioned above are not defined in this work as relevant field data in publications are rare. And available data remain proprietary. An up-to-date literature review suggests that these observations are not unusual. For example, Su (2016) encountered the same situation in his work. To verify the correctness of the research results, we compare this new work against previous studies regarding the strata movement induced by mining activities and the stability of oil/gas wells, methane capture boreholes, GGVs in gassy coal seams, as well as wellbore/casing failure induced by reservoir compaction in the petroleum industry.

4.1. Overburden movement due to longwall mining and reservoir compaction

Longwall mining causes various deformations to the overlying strata, including stretching, bending, shearing, bed separation, subsidence and compression. However, different deformations dominate in different zones. For example, overlying strata are mainly deformed by bending and sinking, tensile separation and compression. While at the edges of the panel or within the overlying strata above the coal pillar, strata

deformations are generally characterized by tension and bending, axial distortion, interlayer shear and compression (Fig. 9). Integrity of wells vertically piercing the coal pillar is affected by these deformations resulting from surface and subsurface subsidence.

Among these deformations, shear is the main pattern of well/wellbore instability and is related primarily to the slippage of layers along weak interfaces within the overburden (Bruno, 1992; Chen et al., 2012; Dusseault et al., 2001; Liang et al., 2014, 2015a; Rostami et al., 2012; Whittles et al., 2007), which has been indicated by many field observations. Horizontal fractures along weak–strong rock layer interfaces play an important role in overburden movement. The generation and propagation of the fractures depend on the type and composition of the rocks overlying the seam (Karacan, 2009). The bedding plane separation probabilities can be predicted using the distances of bedding planes to the extracted coal seam and the thicknesses of neighboring layers, as well as the thickness of the thick and strong rock layer, which is called "bridge layer" (Karacan and Goodman, 2009; Palchik, 2005). Specifically, the probability of bedding plane separation along rock layer interfaces decreases with increasing height above the coal seam and with increasing thickness of the bridge layer. Palchik (2005, 2010) also noted that separations at the interfaces and formation of fractures maybe restrained by the bridge layer.

Similar to the compaction of a longwall gob, reservoir compaction during oil/gas extraction generates high shear stresses in the overburden material near the flanks of the reservoir. Through field observations, Bruno (1992) and Dusseault et al. (2001) found that shear and bending failures of wells often occur within the overburden structure above the flanks/shoulders of the reservoir. This scenario is similar to deep wells traversing longwall pillars, which outline and flank each LWP. The strata above the longwall pillar are less fractured compared to those overlying the gob. However, strata above the longwall pillar experience shearing along bedding planes as they are deflected over the edges of the extracted LWP (Hasenfus et al., 1988).

In this work, we find that apart from mechanical properties of the interfaces and strata, layer thickness and spacing between the coal seam and the stratum/interface are involved as secondary factors in controlling well deformation. Specifically, (1) various deformations (horizontal shear displacement and vertical compression occur at interfaces, axial distortion and the horizontal and vertical strains occur within strata) of the well generally increase as the spacing between the stratum/interface and the coal seam decreases, (2) a large shear displacement is more likely to occur at the interface of SHS strata structures comprising a hard and thick layer (the key-stratum) than at the weak interface alone, and (3) the vertical compression at the interface below the key-stratum dominates the total amount of compression in the overlying strata. These are substantially similar to results of Karacan and Goodman (2009) and Palchik (2005), all of which reflect the impacts of strength properties of interfaces/strata, thickness of the layer and distance between the coal seam and the stratum/interface on the magnitude and distribution of deformation induced by mining activities.

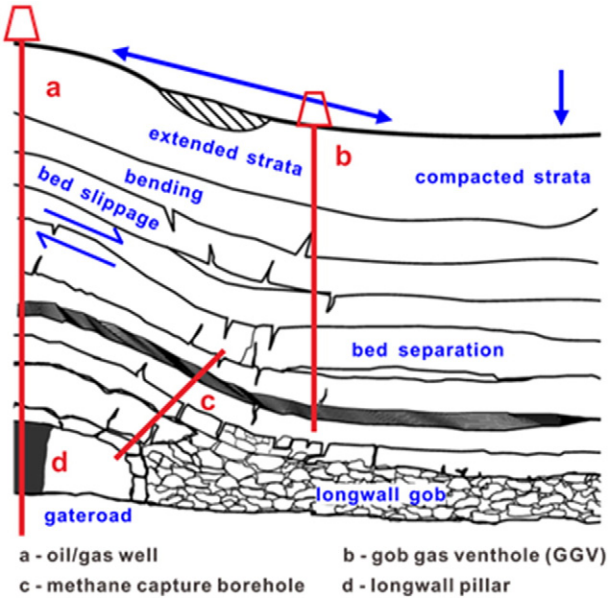

Fig. 9. Schematic of various deformations of the overlying strata around a LWP and locations of deep oil/gas wells, methane capture boreholes and GGVs (modified from Schatzel et al., 2012).

4.2. Deformation of wells/boreholes subject to longwall mining

Existing studies have evaluated axial strains along well trajectories for longwall mining around a gas well at the Cumberland Mine in Pennsylvania (Luo et al., 1999; Scovazzo and Russell, 2013); deformations around a CNX well (Scovazzo and Russell, 2013); strains, displacements and distortions around a two dimensional longwall section both with and without delamination and for a horizontal surface (Rostami et al., 2012); impacts of incised topography and coal seam burial depth (Liang et al., 2014); wellbore failure induced by reservoir compaction in the Gulf of Mexico (Abou-Sayed et al., 2004); stability of methane capture boreholes around a LWP (Whittles et al., 2007); and stability of GGVs (Liu et al., 2005). The background for each study and the areas of overlap between them are tabulated in Tables 3 and 4. Before we compare and contrast these studies, some points should be noted. According to Rostami et al. (2012), "homogeneous" refers to homogeneous strata without a deformability contrast between alternating layers; "layered" refers to the case of alternating 10 m thick monolithic beds of alternating high and low moduli under conditions that neglect delamination or shear slip (bonded interface). In these two scenarios the shear offset (ΔU) is equal to the bed thickness multiplied by local distortion (shear strain). In Liang et al. (2014) and this study, "with delamination" refers to the cases with bed-delamination and shear slip for geometries. Moreover, in this most recent study the effects of strata combination structures on the magnitude and distribution of various well deformations are also taken into proper account.

Seam depth, thickness and pillar width are congruent in all the studies (Table 3) except for the case where the topography effect is considered and the seam is at a depth of approximately 600 m including the hill thickness (300 m). In prior work (Luo et al., 1999), vertical strains of a well caused by shortening are predicted to be 6×10^{-5} after removal of the first panel and are magnified 10 times (6×10^{-4}) as the second panel is mined. However, these are significantly smaller than those caused by subsidence (Liang et al., 2014; Rostami et al., 2012; this study) which are of the order of 10^{-4}–10^{-3}. Similarly, maximum shear offsets (Scovazzo and Russell, 2013) are of the order of 1.2–2.3 cm for various thicknesses of stiff beds (0.5–3 m), and are separately limited to ± 10 cm and ± 20 cm in prior studies (Liang et al., 2014; Rostami et al., 2012) and this study, in which layers are 0.3–25 m thick. Thus, combining with the thicknesses of adjacent layers above and below the interfaces (Table 1 and Fig. 4), it is surmised that shear offset is positively correlated with bed thickness. Compared to the case where delamination and slip on bed interfaces are not suppressed (Liang et al., 2014 and this study), peak lateral shear offsets approximately double under the effect of weak contacts (horizontal ground surface; Table 3), and further increase as influenced by incised topography (incised topography; Table 3). Shear strains in the strata (Liang et al., 2014 and this study) are reduced over the layered case (Rostami et al., 2012) and it is surmised that bedding slip dissipates the magnitudes within the solid media. Strains in lateral extension and vertical compression decrease due to bedding slip and separation, respectively; while strains in lateral compression and vertical extension increase (Liang et al., 2014; Rostami et al., 2012). When the effects of strata-combination-structures are considered (this study), peak strains both in the lateral and vertical compression change slightly compared to the case

Table 3
Comparison of various deformational modes of wells subject to longwall mining with previous studies.

Study performed by		Burial depth/m	Seam thickness/m	Pillar width/m	First mined panel				Second mined panel			
					Shear offset ΔU/cm	Shear strain/ε_{xy}	Lateral strain/ε_{xx}	Vertical strain/ε_{yy}	Shear offset ΔU/cm	Shear strain/ε_{xy}	Lateral strain/ε_{xx}	Vertical strain/ε_{yy}
Luo et al., 1999		307	1.9	56	–	–	–	−6 E-5	–	–	–	−6 E-4
Su, 2009 (Scovazzo and Russell, 2013)		315	1.7	65	–	–	–	–	1.2– 2.3	–	–	–
Rostami et al., 2012	Homogeneous	300	2.0	50	0–1.2	0–1 E-3	−1–4 E-4	−2–0 E-4	0–3	0–3 E-3	0–2 E-3	−2–0E-3
	Layered	300	2.0	50	−2–7	−2–7 E-3	−1–8 E-3	−5–2 E-3	−8–6	−8–6 E-3	−1–8 E-3	−8–10 E-3
Liang et al., 2014 (with delamination)	Horizontal	300	2.0	50	3–17	−1–22 E-4	−26–52 E-4	−15–149E-4	−17–13	−22–23 E-4	−47–77 E-4	−22–164 E-4
	Incised	300 + 300	2.0	50	2–22	−3–15 E-4	−3–5 E-3	−2–0 E-3	−20–15	−23–13 E-4	−6–10 E-3	−3–1 E-3
This study (with delamination)	with effects of strata combination structures been under consideration	305.3	2.0	50	3–14	−1–13 E-4	−25–80 E-4	−15–6 E-4	−13–10	−24–14 E-4	−43–116 E-4	−24–7 E-4

where the formation is uniformly alternating and comprising ~10 m thick alternating shale and sandstone layers (Liang et al., 2014). These peak strains all occur within the seam or in the lower part of the immediate roof. While the largest lateral extensional strains increase and the peak vertical extensional strains decrease drastically due to the presence of the key-stratum.

We also make a comparison of casing/borehole strains between this new work and previous studies regarding the stability of methane capture boreholes and GGVs in gassy coal seams, and casing/wellbore failure induced by reservoir compaction in the petroleum industry. Statistical data from these previous studies are tabulated in Table 4, in which "FTD" and "MPR" separately refer to field test data and numerical model predicted results that have been confirmed by field observation after 6 years production; "FEMW" and "FEMWO" separately indicate the hybrid finite element predicted results both with and without the consideration of casing, cement and rock rigidity; and "GM" and "GDF" separately represent results predicted from a geomechanical model and calculated from the Gaussian distribution function.

Vertical strains induced by reservoir compaction and resulting from pore collapse of weak reservoir rocks after 5–6 years production are larger than those of wells in this work by over one order of magnitude. Specifically, the vertical compressional and tensional strains of casings are approximately 16–29 and 10–16 times, respectively, as large as those of wells subject to longwall coal mining (i.e. this study, after the twin flanking panels are both mined) (Table 4). It is surmised that the accumulated larger non-uniform subsurface subsidence due to the deep reservoir (>5000 m) and long term (>5 years) production accounts for this difference in magnitude of vertical strains. However, the horizontal compressional casing strains are much less than those of wells in this study, accounting for 5%–47% of the later; and the horizontal tensional casing strains are also less compared to those of wells in this work, accounting for 49%–95% of the later.

The greatest vertical compressional strain of GGVs calculated from the Gaussian distribution function is of the order of −74 E-4 (Liu et al., 2005), which is between five and three times that of wells in this work after the twin panels flanking the coal pillar are sequentially removed. This might imply more intense movement and deformation of strata above the longwall gob compared with that within the strata above the coal pillar (Fig. 9). Certainly, the seam depth, mining height and mechanical properties of the overlying strata and interfaces could also dictate the magnitude of the deformation of the wells/boreholes. To be noted is that the axial distribution of vertical compressional strain of the GGVs, calculated from the Gaussian distribution function, is roughly similar to that of wells in this work (Fig. 8). However, the Gaussian model cannot accommodate the impacts of lithology and bed thickness.

Similarly, shear strains of methane capture boreholes drilled from the tailgate roadway and across the shallow roof (Fig. 9) in a UK active LWP located in the Parkgate coal seam at a depth of 770 m (Whittles et al., 2007) are much greater than those of wells drilled through a longwall pillar. This is due principally to the comprehensive effects of severe shear deformation within the shallow overburden at the inboard edges of the panel (Fig. 9) and the deeper seam depth. Magnitudes of shear strains of the methane capture boreholes (of the order of 10^{-2}–10^{-1}) are nearly 50–92 times those of wells in this work (of the order of 10^{-3}).

4.3. Drilling path optimization for wells penetrating the longwall pillar

We conduct a thorough integrated evaluation of various deformations of the five well trajectories analyzed in the previous section,

Table 4
Statistical variations of strains of wellbores, methane capture boreholes and GGVs from previous studies.

Study conducted by			Reservoir/seam depth/m	Seam thickness/m	Strains		
Abou-Sayed, et al., 2004	Wellbore failure induced by reservoir compaction	Case 1	5182	–	Vertical strain (FTD)		−38–11 E-3
		Case 2	6096	–	Vertical strain (MPR)		−67–8 E-3
		Case 3	6096	–	Vertical strain	FEMWO	−52–1 E-3
						FEMW	−41–1 E-3
						GM	−70–7 E-3
					Horizontal strain	FEMWO	−2–76 E-4
						FEMW	−2–57 E-4
						GM	−2–11 E-3
Liu, et al., 2005	GGVs		475	2.5	Vertical compressional strain (GDF)		−74 E-4
Whittles, et al., 2007	Methane capture boreholes		770	2.0	Shear strain (GM)		−12–2 E-2
This study	Oil/gas wells (after the twin LWPs are both removed)		305.3	2.0	Vertical strain		−24–7 E-4
					Horizontal strain		−43–116 E-4
					Shear strain		−24–14 E-4

especially the horizontal shear offset which jeopardizes well integrity the most. Trajectory W3 is the recommended drilling path for the well. That is, positioning the well closer to the rib of the second mined panel favors well integrity. It is speculated that, based on our numerical modeling results, part of the deformation of the wellbore in the overlying strata can be recovered and that some deformations cannot be restored (and may even intensify) after the twin panels flanking the coal pillar are sequentially removed. Although the authors did not discuss the relation between the position of the well within the coal pillar and its stability, supporting evidence for this viewpoint is available from field engineering practice (Peng et al., 2003). Fig. 10 shows the layouts of the gateroad system of both the stable well case and that of the failed well. For the successful case (Fig. 10 (a)), the gas well is located closer to the rib of the second advancing panel (13.2 m out from the pillar-center for a 56.9 m wide three-entry longwall pillar) (Table 5) and no casing destruction was observed after the twin flanking panels were sequentially removed. While for the case of failure (Fig. 10 (b)), the gas well is located closer to the rib of the first mined panel (12.3 m out from the pillar-center for a 56.0 m wide three-entry longwall pillar) (Table 5) and plastic failure was observed on the inner tubing of the well after panel 2 was mined.

5. Conclusions

Increased demand for energy encourages the exploitation of unconventional hydrocarbon resources. In areas where the overlaying coal and deep hydrocarbon resources coexist, longwall mining may inevitably damage the transiting wells; therefore, maintaining the stability of these wells has become a significant issue impeding the co-extraction of these resources. This paper investigates the effect of strata combination structures on the magnitude and distribution of various well deformations, and explores the optimal well drilling path favoring the well integrity. The main conclusions are as follows:

(1) The effects of various combinations of strata on well deformation (including horizontal shear offset and vertical compression occurring at the weak interfaces between alternating layers, and the axial distortion, horizontal and vertical tension and compression occurring within the strata) lie essentially in the mechanical properties of the interfaces and strata. The stratum thickness and the spacing between the coal seam and the stratum/interface are also involved as secondary factors in controlling well deformation. Longwall mining-induced interfacial shear displacements at interfaces between a monolithic rigid bed (e.g. the key-stratum) and its immediate overlaying and underlaying soft beds (e.g. shales/mudstones, SHS strata structure), especially at the interface sandwiched above by a thick stiff layer and below by a thick soft layer, are much larger than those at interfaces with simply low stiffness. However, wells are not susceptible to large horizontal shear slippage at interfaces between one thin soft interlayer and the stiff beds directly above and below (HSH strata structure), and between the topsoil and its underlaying bedrock. Well deformations arising both at interfaces and within layers all significantly intensify in the vicinity of the mined seam. Wells in such areas are therefore at high risk of instability.

(2) Different types of strata combinations (the topsoil-bedrock, HSH, and SHS strata structures) influence the magnitude and distribution of various well deformations to varying extents. The horizontal and vertical strains in the topsoil change gradually then vary abruptly at the interface between the topsoil and its underlaying bedrock. Wells in the upper part of the topsoil are subject to horizontal tension after either one or both panels are removed, while the lower part is compressed. Lateral strains are dominated by tension in the upper part of stiff beds (e.g. the upper part of the bedrock, the key stratum, and the sandstone directly below the thin weak interlayer) which directly lie beneath the soft beds. The larger lateral tensile strains are for wells in the shallow roof (~5–20 m above the seam). While the larger lateral

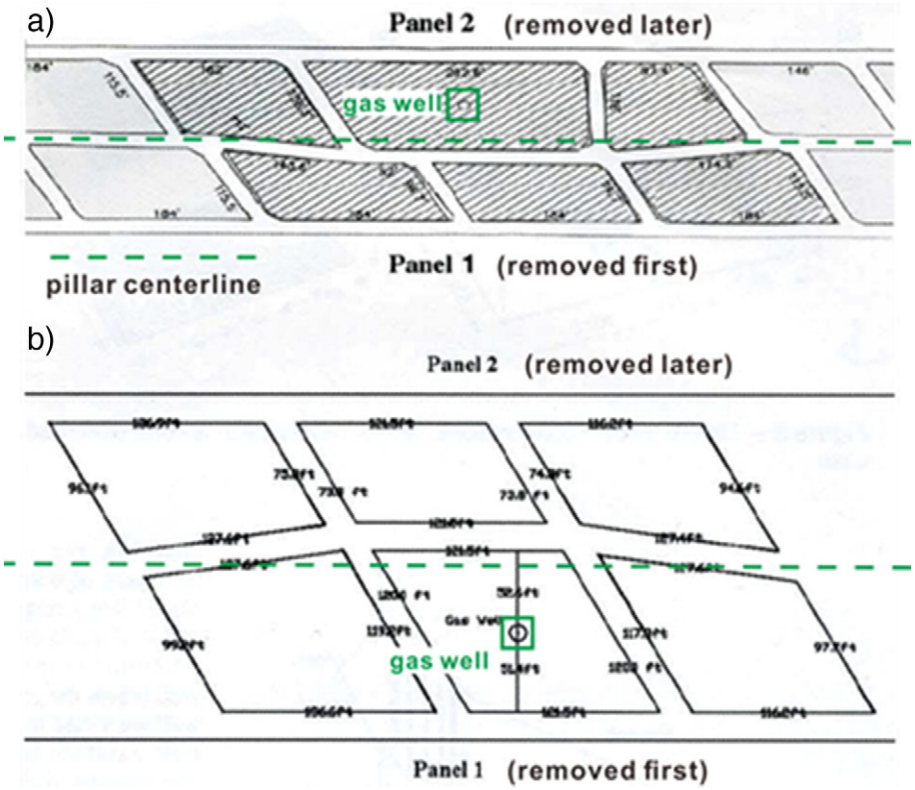

Fig. 10. The spatial relationship between the gas well and the twin LWPs flanking the longwall coal pillar: (a) successful case and (b) failure case. (modified from Peng et al., 2003).

Table 5
Comparison of longwall pillar configuration and well trajectory locations between this work and two field cases.

Study conducted by		Pillar configuration (yield pillar + gateroad + barrier pillar)		Panel width/m	Seam burial depth/m	Mining height/m	Entries width/m	Width of the barrier pillar the gas well piercing/m	Off center distance/m
Peng, et al., 2003	Successful case	3-entry system	21.5 + 4.9 + 30.5 = 56.9 m	305	159	2.4	4.9	30.5	13.2
	Failed case		19.3 + 5.0 + 31.7 = 56 m	274	287	1.9	5.0	31.7	−12.3
This study		3-entry system	15 + 5.0 + 30 = 50 m	370	305.3	2.0	5.0	30.0	7.5

Note: For "off center distance", negative and positive values represent that the well is drilled off the pillar centerline and close to the first and second mined panel, separately.

compressive strains are for wells in the vicinity of the seam (within ~5 m above and below the seam) and peak in the coal seam.

(3) Longitudinal well deformation in soft strata is dominated by compression especially in the upper part of the layer. Vertical tension plays a dominant role in well deformation in stiff/hard layers, especially in their lower reaches. The shallow topsoil has a greater vertical well deformation that is dominated by tension. The vertical interfacial compression is larger at interfaces below the key-stratum, peaking at the interface between the coal seam and its immediate roof. The key-stratum behaves like a barrier layer, preventing the overlying strata from bending and subsiding and preventing mining-induced damage from propagating upwards. Small increases in vertical interfacial compression are detected at interfaces between 1) the key-stratum and its immediately underlying soft layer, 2) a thin weak stratum and its immediately overlying hard layer, and 3) topsoil and the bedrock after either one or both panels are removed. Since the strata beneath the topsoil alternate as soft mudstones and stiff sandstones, the axial distortion of wells traversing these strata fluctuate. Well distortion within the soft strata exceeds that in the stiff strata, generally reaching 3 to 5 times the distortion of the latter, and reaching a peak distortion of $\sim 10^{-3}$ for the well in the shallow roof (~8 m above the seam).

(4) After extraction of the twin LWPs, the interfacial horizontal shear offsets and the intra-formational axial distortion of the well rebounds to some extent in the upper part of the overlying strata, due to the symmetry of mining geometry. However, in the seam and its shallow roof (within 30 m), these deformations intensify because of the intense influence of the mining of the second LWP. The intra-formational vertical and horizontal strains of the well (for most of the length of the well) increase further after the extraction of the second LWP. And this increment increases sharply as the spacing between the stratum and the coal seam decreases.

(5) In the cross section of the pillar, various deformations of wells W1 and W5, which traverse the edges of the longwall pillar, are greater to varying extents than those of wells W2-W4 after the twin LWPs are sequentially excavated. The maximum lateral shear offset of well W3 is 97.5 mm, which is the least among the five candidate paths of wells in the entire mining cycle of the twin panels. Well W2, which is closest to the pillar center and traverses the edge of the barrier pillar, has the lowest interfacial compression (−488 mm), but this is close to that of well W3 (−498 mm). In addition, there is a prominent increase in the axial distortion and lateral tensile strain for well W2 in the upper part of the key-stratum after either one or both panels are removed. Thus, through an integrated consideration of various deformations of these five wells, especially the lateral shear deformation which threatens well integrity the most, trajectory W3 (deviating suitably from the pillar centerline and close to the second mined panel) is the recommended drilling path for the well. Supporting evidence for this viewpoint is apparent from field engineering practice.

(6) Spatially, magnitudes of various deformations of strata directly over the gob, pillars and edges of the panel differ. Due to the larger subsidence of overlying strata above the gob compared with that occurring within the overlying strata above the pillar, vertical compressive strains of the GGVs are usually greater than those of wells in the overlying strata of the pillar. As for methane capture boreholes sidetrack drilled from the tailgate and across the shallow roof of an LWP, the shear strains of boreholes occur as the strata in the overlying edges of the panel bend, tilt and subside during the panel-advance cycle and these are far larger than those for wells piercing the pillar. While for the hydrocarbon wells, the vertical casing strains (both compressive and extensile) induced by reservoir compaction as a result of pore collapse of weak reservoir rocks after long-term production are generally larger than those of wells penetrating the longwall pillars by more than one order of magnitude.

Acknowledgements

Financial support for this work, provided by China Postdoctoral Science Foundation (2015M581893), the National Natural Science Foundation of China (Nos. 41602174 and 51674248), the Fundamental Research Funds for the Central Universities (2015XKZD04), and the Priority Academic Program Development of Jiangsu Higher Education Institutions (PAPD), is gratefully acknowledged.

References

Abou-Sayed, A.S., Meng, F.H., Wang, G., 2004. Compaction-Induced Wellbore Failure and Fault Instability: A Hybrid Approach. American Rock Mechanics Association.
Bruno, M.S., 1992. Subsidence-induced well failure. SPE Drill. Eng. 7 (2), 148–152 (SPE-20058-PA).
Chen, J., Wang, T., Zhou, Y., Zhu, Y., Wang, X., 2012. Failure modes of the surface venthole casing during longwall coal extraction: a case study. Int. J. Coal Geol. 90–91, 135–148.
Dodson, J.K., 2004. Gulf of Mexico 'trouble time' creates major drilling expenses. Offshore 64 (1).
Dusseault, M.B., Bruno, M.S., Barrera, J., 2001. Casing shear: causes, cases, cures. SPE 72060. SPE Drill. Complet. 16 (2), 98–107.
Fan, G.W., Zhang, D.S., 2015. Mechanisms of aquifer protection in underground coal mining. MineWater Environ 34, 95–104.
Ghazvinian, A.H., Taghichian, A., Hashemi, M., Mar'Ashi, S.A., 2010. The shear behavior of bedding planes of weakness between two different rock types with high strength difference. Rock Mech. Rock. Eng. 43, 69–87.
Hasenfus, G.J., Johnson, K.L., Su, D.W.H., 1988. A hydrogeomechanical study of overburden aquifer response to longwall mining. Proceeding of 7th International Conference on Ground Control in Mining. West Virginia University, Morgantown, pp. 149–162.
Huang, H., 2010. Study on geological theories of stress relief coalbed methane drainage from the distant protected seam by vertical surface wells and their application in Huainan coal mine area. Ph.D. Thesis. China University of Mining and Technology, Xuzhou, China.
Itasca Ltd., 2002. FLAC2D, User's Manual. Itasca Consulting Group, Inc.
Karacan, C.Ö., 2009. Reservoir rock properties of coal measure strata of the Lower Monongahela Group, Greene County (Southwestern Pennsylvania), from methane control and production perspectives. Int. J. Coal Geol. 78, 47–64.
Karacan, C.Ö., 2015. Analysis of gob gas venthole production performances for strata gas control in longwall mining. Int. J. Rock Mech. Min. Sci. 79, 9–18.

Karacan, C.Ö., Goodman, G., 2009. Hydraulic conductivity changes and influencing factors in longwall overburden determined by slug tests in gob gas ventholes. Int. J. Rock Mech. Min. Sci. 46, 1162–1174.
Karacan, C.Ö., Diamond, W.P., Esterhuizen, G.S., Schatzel, S.J., 2005. Numerical analysis of the impact of longwall panel width on methane emissions and performance of gob gas vent holes. Proc. Int. Coalbed Methane Symposium (Paper 0505, Tuscaloosa, AL. 18–19 May. 28 pages).
Karacan, C.Ö., Esterhuizen, G.S., Schatzel, S., Diamond, W.P., 2007. Reservoir simulation-based modeling for characterizing longwall methane emissions and gob gas venthole production. Int. J. Coal Geol. 71, 225–245.
Karacan, C.Ö., Ruiz, F.A., Cotè, M., Phipps, S., 2011. Coal mine methane: a review of capture and utilization practices with benefits to mining safety and to greenhouse gas reduction. Int. J. Coal Geol. 86, 121–156.
Liang, S., 2015. Study on the stability of vertical shale gas wells penetrating longwall mining areas. Ph.D. Thesis. China University of Mining and Technology, Xuzhou, China.
Liang, S., Elsworth, D., Li, X., Yang, D., 2014. Topographic influence on stability for gas wells penetrating longwall mining areas. Int. J. Coal Geol. 132, 23–36.
Liang, S., Elsworth, D., Li, X., Fu, X., Yang, D., Yao, Q., Wang, Y., 2015a. Dynamic impacts on the survivability of shale gas wells piercing longwall panels. Journal of Natural Gas Science and Engineering 26, 1130–1147.
Liang, S., Li, X., Yao, Q., Yang, D., 2015b. Influence of weak interlayer contacts on the stability of shale gas wells transiting minable coal seams. Journal of Mining and Safety Engineering 32, 471–477 (In Chinese with English abstract).
Liu, Y.Z., Lu, T.K., Yu, H.Y., 2005. Surface boreholes for drainage of goaf gas and its stability analysis. Chin. J. Rock Mech. Eng. 24, 4982–4987 (In Chinese with English abstract).
Lu, C.P., Liu, Y., Wang, H.Y., Liu, P.F., 2016. Microseismic signals of double-layer hard and thick igneous strata separation and fracturing. Int. J. Coal Geol. 160, 28–41.
Luo, Y., Peng, S., Zhang, Y., 1999. Analysis of the Observed Failure on the Inner Tubing of Gas Well W-510 Below the Coal Seam. College of Engineering and Mineral Resources, West Virginia University (May 24).
Luo, Y., Peng, S., Zhang, Y., Mordy, K., 2002. Techniques for assessing the effects of longwall mining on gas and oil wells. 2002 SME Annual Meeting and Exhibit, pp. 25–27 February.
Majdi, A., Hassani, F.P., Nasiri, M.Y., 2012. Prediction of the height of destressed zone above the mined panel roof in longwall coal mining. Int. J. Coal Geol. 98 (1), 62–72.
Miyazaki, B., 2009. Well Integrity: An Overlooked Source of Risk and Liability for Underground Natural Gas Storage. Lessons Learned from Incidents in the USA. vol. 313. Geological Society London Special Publications, pp. 163–172.
Palchik, V., 2003. Formation of fractured zones in overburden due to longwall mining. Environ. Geol. 44, 28–38.
Palchik, V., 2005. Localization of mining-induced horizontal fractures along rock layer interfaces in overburden: field measurements and prediction. Environ. Geol. 48, 68–80.
Palchik, V., 2010. Experimental investigation of apertures of mining-induced horizontal fractures. Int. J. Rock Mech. Min. Sci. 47 (3), 502–508.
Peng, S., Morsey, K., Zhang, Y., Luo, Y., Heasley, K., 2003. Technique for assessing the effects of longwall mining on gas wells-two case studies. Transactions-society for mining metallurgy and exploration incorporated 314, 107–115.
Preusse, A., 2001. Effect of face advance rates on the characteristics of subsidence processes associated with US and Germany longwall mining. 20th International Conference on Ground Control in Mining, Morgantown, WV, pp. 140–148.
Qian, M., 1996. Theoretical study of key stratum in ground control. J. China Coal Soc. 21, 225–230.
Rice, G.S., Hood, O.P., 1913. Oil and Gas Wells Through Workable Coal Beds (No. BM-BULL-65). Bureau of Mines, Washington, DC (USA).
Richard, R., Randolph, J., Zipper, D., 1990. High extraction mining, subsidence, and Virginia's water resources. chapter 4. Subsidence Effects on Water Resources. Virginia Center for Coal & Energy Research. Virginia Polytechnic Institute and state University, Virginia, pp. 17–20.
Rostami, J., Elsworth, D., Watson, R., 2012. Study of Borehole Stability for Gas Wells in Longwall Mining Areas (Report Submitted to Range Resources).
Rueda, J., Noreña, N., Oliveira, M., Roehl, D., 2014. Numerical models for detection of fault reactivation in oil and gas fields. 48th US Rock Mechanics Conference (ARMA 2014), pp. 1–8.
Schatzel, S.J., Karacan, C.Ö., Dougherty, H., Goodman, G.V.R., 2012. An analysis of reservoir conditions and responses in longwall panel overburden during mining and its effect on gob gas well performance. Eng. Geol. 127, 65–74.
Scovazzo, V.A., Russell, P.M., 2013. Industry research into gas and oil well protective coal pillar design. 32nd International Conference on Ground Control in Mining, Morgantown, WV, pp. 45–52.
Su, W.H., 2016. Effects of longwall-induced stress and deformation on the stability and mechanical integrity of shale gas wells drilled through a longwall abutment pillar. 35th International Conference on Ground Control in Mining, Morgantown, West Virginia, pp. 1–7.
Sun, H., 2008. Study on the deformation fracture mechanism of the surface borehole with the excavation disturbance. Ph.D. Thesis. Chongqing University, Chongqing, China.
Vidic, R.D., Brantley, S.L., Vandenbossche, J.M., Yoxtheimer, D., Abad, J.D., 2013. Impact of shale gas development on regional water quality. Science 340 (6134), 1235009.
Wang, J., Wei, X., Chen, S., 2012. Fracture and seepage characteristics in the floor strata when mining above a confined aquifer. J. China Univ. Min. Technol. 41, 536–542 (In Chinese with English abstract).
Wang, J., Li, H., Chen, P., 2014. Exploration and practice on treatment technology of depleted oil wells in coal mine. Coal Technology 33, 262–265 (In Chinese with English abstract).
Wang, Y., Watson, R., Rostami, J., Wang, J., Limbruner, M., He, Z., 2013. Study of borehole stability of Marcellus shale wells in longwall mining areas. J. Pet. Explor. Prod. Technol. 1–13.
Whittles, D.N., Lowndes, I.S., Kingman, S.W., Yates, C., Jobling, S., 2006. Influence of geotechnical factors on gas flow experienced in a UK longwall coal mine panel. Int. J. Rock Mech. Min. Sci. 43, 369–387.
Whittles, D.N., Lowndes, I.S., Kingman, S.W., Yates, C., Jobling, S., 2007. The stability of methane capture boreholes around a long wall coal panel. Int. J. Coal Geol. 71, 313–328.
Xu, H., Sang, S., Han, J., Huang, H., Cheng, Z., Ren, B., 2011. Relationship between rock mass structure and stability of surface well for released coal gas. Journal of Mining and Safety Engineering 28, 90–95 (In Chinese with English abstract).
Yan, C., Deng, J., Yu, B., 2013. Wellbore stability in oil and gas drilling with chemical-mechanical coupling. Sci. World J. 2013.
Yun, S., 2014. Analysis on the impacts of simultaneous extraction of coal and natural gas on coal mine safety. Science and Technology Information, Heilongjiang 57 (In Chinese).
Zeynali, M.E., 2012. Mechanical and physico-chemical aspects of wellbore stability during drilling operations. J. Pet. Sci. Eng. 82-83, 120–124.
Zhai, C., Xu, Y., Xiang, X., Yu, X., Zou, Q., Zhong, C., 2015. A novel active prevention technology for borehole instability under the influence of mining activities. Journal of Natural Gas Science and Engineering 27, 1585–1596.
Zhang, J., Lang, J., Standifird, W., 2009. Stress, porosity, and failure-dependent compressional and shear velocity ratio and its application to wellbore stability. J. Pet. Sci. Eng. 69 (3), 193–202.
Zabetakis, M.G., Moore Jr., T.D., Nagel, A.E., Carpetta, J.E., 1972. Methane Emission in Coal Mines: Effects of Oil and Gas Wells. 7658. US Bureau of Mines Report of Investigations.